

# Cerebellar Activation Deficits in Schizophrenia During an Eyeblink Conditioning Task

Nancy B. Lundin<sup>1,2,○</sup>, Dae-Jin Kim<sup>1</sup>, Rachel L. Tullar<sup>1</sup>, Alexandra B. Moussa-Tooks<sup>1,2,3,○</sup>, Jerilyn S. Kent<sup>4</sup>, Sharlene D. Newman<sup>1,5</sup>, John R. Purcell<sup>1,2</sup>, Amanda R. Bolbecker<sup>1,6,○</sup>, Brian F. O'Donnell<sup>1,2,6</sup>, and William P. Hettrick<sup>\*,1,2,6</sup>

<sup>1</sup>Department of Psychological and Brain Sciences, Indiana University, Bloomington, IN, USA; <sup>2</sup>Program in Neuroscience, Indiana University, Bloomington, IN, USA; <sup>3</sup>Department of Psychiatry and Behavioral Sciences, Vanderbilt University School of Medicine, Nashville, TN, USA; <sup>4</sup>Department of Psychiatry and Behavioral Sciences, University of Minnesota Medical School, Minneapolis, MN, USA; <sup>5</sup>Alabama Life Research Institute, University of Alabama, Tuscaloosa, AL, USA; <sup>6</sup>Department of Psychiatry, Indiana University School of Medicine, Indianapolis, IN, USA

\* To whom correspondence should be addressed; 1101 East Tenth Street, Bloomington, IN 47405, USA; tel: 812-855-2620, fax: 812-856-4544, e-mail: [whetrick@indiana.edu](mailto:whetrick@indiana.edu)

The cognitive dysmetria theory of psychotic disorders posits that cerebellar circuit abnormalities give rise to difficulties coordinating motor and cognitive functions. However, brain activation during cerebellar-mediated tasks is understudied in schizophrenia. Accordingly, this study examined whether individuals with schizophrenia have diminished neural activation compared to controls in key regions of the delay eyeblink conditioning (dEBC) cerebellar circuit (eg, lobule VI) and cerebellar regions associated with cognition (eg, Crus I). Participants with schizophrenia-spectrum disorders ( $n = 31$ ) and healthy controls ( $n = 43$ ) underwent dEBC during functional magnetic resonance imaging (fMRI). Images were normalized using the Spatially Unbiased Infratentorial Template (SUIT) of the cerebellum and brainstem. Activation contrasts of interest were “early” and “late” stages of paired tone and air puff trials minus unpaired trials. Preliminary whole brain analyses were conducted, followed by cerebellar-specific SUIT and region of interest (ROI) analyses of lobule VI and Crus I. Correlation analyses were conducted between cerebellar activation, neuropsychological test scores, and psychotic symptom scores. In controls, the largest clusters of cerebellar activation peaked in lobule VI during early dEBC and Crus I during late dEBC. The schizophrenia group showed robust cortical activation to unpaired trials but no significant conditioning-related cerebellar activation. Crus I ROI activation during late dEBC was greater in the control than schizophrenia group. Greater Crus I activation correlated with higher working memory scores in the full sample and lower positive psychotic symptom severity in schizophrenia. Findings indicate functional cerebellar abnormalities in

schizophrenia which relate to psychotic symptoms, lending direct support to the cognitive dysmetria framework.

*Key words:* psychosis/cerebellum/associative learning/functional magnetic resonance imaging

## Introduction

The cognitive dysmetria theory of schizophrenia posits that patterns of cerebellar dysconnectivity to cerebral brain regions may contribute to the discoordination of motor and cognitive functioning.<sup>1</sup> In broad support of this theory, abnormalities in the cerebellar node of this circuit in individuals with psychotic disorders have been reported, including abnormalities in grey matter volume,<sup>2-4</sup> white matter integrity,<sup>5-8</sup> and functional activation and connectivity with cerebral regions during tasks<sup>9-11</sup> and resting state.<sup>12-16</sup> Moreover, studies have reported deficits in individuals with psychotic disorders across a wide range of behavioral tasks indexing cerebellar-dependent motor and timing functions. These deficits are typically characterized by decreased total learning and learning rates, impaired adaptation, and higher performance variability compared to nonpsychiatric control groups on tasks including postural sway,<sup>17,18</sup> self-paced finger tapping,<sup>11,19</sup> prism adaptation,<sup>20,21</sup> temporal bisection,<sup>22-24</sup> and motor sequence learning.<sup>25,26</sup> However, neural activation during cerebellar-mediated tasks is understudied in schizophrenia.

Delay eyeblink conditioning (dEBC) is a well-established and highly translational cerebellar-mediated

classical conditioning paradigm in which individuals with schizophrenia frequently exhibit impaired task performance,<sup>27</sup> making it an ideal candidate for studying cerebellar function in psychotic illness. In dEBC, a neutral stimulus (which becomes a conditioned stimulus; CS) such as a tone precedes and coterminates with an air puff (unconditioned stimulus; US) to the eye, which elicits a reflexive eyeblink response (unconditioned response; UR). Over repeated pairings, associative learning typically occurs via development of a conditioned response (CR) in the form of anticipatory blink activity to the tone prior to the air puff onset. There is a robust body of evidence indicating reduced generation of CRs during dEBC in schizophrenia,<sup>28–31</sup> although studies have occasionally reported opposing findings.<sup>32</sup> Lower dEBC CR rates have also been observed across the psychosis spectrum (eg, schizotypal personality disorder,<sup>33</sup> first-degree relatives of individuals with schizophrenia<sup>34</sup>) as well as in other neurodevelopmental disorders with known cerebellar abnormalities,<sup>35</sup> indicating that impaired dEBC may broadly serve as a behavioral marker of cerebellar circuit dysfunction.

Delay EBC is an ideal assay of cerebellar integrity because of its well characterized cerebellar circuits in nonhuman animal studies.<sup>36</sup> Research suggests that the anterior lateral portion of the interposed deep cerebellar nuclei is a critical site of formation and storage of the memory trace for the conditioned dEBC response.<sup>37,38</sup> Evidence also suggests an important role of hemispheric lobule VI of the cerebellar cortex in dEBC. Anatomical findings indicate that lobule VI projects axons to the interposed nuclei and also receives projections from olivary climbing fibers involved in the US dEBC pathway as well as the pontine mossy fibers involved in the CS dEBC pathway.<sup>39</sup> Moreover, intracellular recording studies have found conditioning-related increases in lobule VI Purkinje cell spiking.<sup>40</sup> Lobule VI damage alters dEBC CRs, although the nature of reported dEBC-related changes are not identical across studies. Some studies have found lobule VI lesions to abolish or initially decrease acquisition of the CR,<sup>41,42</sup> yet others have solely found such lesions to alter response timing or amplitude.<sup>38,43</sup> Largely aligning with the nonhuman animal literature, human functional magnetic resonance imaging (fMRI) studies have shown that the most prominent cerebellar regions activated during paired dEBC trials compared to rest or unpaired trials are lobule VI, Crus I, and the interposed and dentate cerebellar deep nuclei, with additional activations reported in lobule VIIIb and the anterior lobe.<sup>44–48</sup>

Despite the large bodies of existing work demonstrating (1) the essential role of the cerebellum in dEBC, (2) cerebellar abnormalities in psychotic disorders, and (3) dEBC deficits in psychotic disorders, very few studies have bridged these literatures by investigating cerebellar activity during dEBC in individuals with psychotic

illness. One positron emission tomography (PET) study found that in contrasts of paired trials minus unpaired trials, individuals with schizophrenia had less regional cerebral blood flow (rCBF) than healthy controls in cerebellar anterior lobules IV and V as well as posterior lobule VI.<sup>31</sup> In a recent dEBC pilot study from our group, whole brain fMRI activation analyses of paired versus unpaired trials revealed a small cluster of activated voxels in the right cerebellum near the deep nuclei in healthy controls that did not reach significance in individuals with schizophrenia.<sup>49</sup> Moreover, in cerebellar-specific analyses, clusters in right lobule VIIIa and right Crus I were inversely associated with negative symptoms in participants with schizophrenia. These provocative findings motivated this larger study which incorporates processing procedures optimized to characterize cerebellar activity. The Spatially Unbiased Infratentorial Template (SUIT) toolbox<sup>50</sup> is ideal for this purpose, as it has improved segmentation and alignment of cerebellar structures than standard whole brain pipelines.

In the present study, individuals with schizophrenia-spectrum disorders and nonpsychiatric controls underwent dEBC during fMRI. Preliminary whole brain analyses were conducted, after which the SUIT processing pipeline was used to isolate and spatially normalize cerebellar activity. Whole cerebellar analyses identified regions associated with early and late stages of dEBC, followed by region of interest (ROI) analyses examining diagnostic group differences in lobule VI given its well documented role in dEBC<sup>36</sup> and Crus I given its associations with higher-order cognitive functions<sup>51</sup> and symptom severity in our pilot study.<sup>49</sup> First, we hypothesized that healthy control participants would exhibit significant cerebellar activation during dEBC, particularly in cerebellar regions such as lobule VI, Crus I, and the deep cerebellar nuclei.<sup>44–48</sup> Second, we hypothesized that individuals with schizophrenia would exhibit diminished cerebellar activation during dEBC compared to controls.<sup>31,49</sup> Finally, we hypothesized that increased posterior cerebellar activation during dEBC would correlate with greater working memory capacity,<sup>52,53</sup> higher processing speed,<sup>33</sup> and lower psychotic symptom severity.<sup>49</sup>

## Methods

### *Participants*

Participants were recruited via newspaper ads, flyers, and hospital referrals from clinics affiliated with Indiana University School of Medicine in Indianapolis, IN, USA. All participants provided informed consent to study procedures approved by the Indiana University Institutional Review Board. Exclusion criteria consisted of history of a serious medical or neurological condition, head injury resulting in a loss of consciousness >5 min, learning disability, current illicit drug use (indicated by a urine drug screen on the date of MRI), current or past

alcohol/drug abuse or dependence (past: within 6 months for the clinical group; lifetime for controls), a history of electroconvulsive therapy, and MRI contraindications. Trained research coordinators and clinical psychology graduate students administered the mood, psychotic, and substance use disorders sections of the Structured Clinical Interview for DSM-IV TR Axis I Disorders (SCID-I)<sup>54,55</sup> to all participants and the paranoid, schizotypal, schizoid, and antisocial personality disorder sections of the SCID-II<sup>56</sup> to participants enrolled as healthy controls. Anxiety disorders were assessed using the Mini International Neuropsychiatric Interview (M.I.N.I.).<sup>57</sup> Medical charts were referenced as necessary to supplement interviews.

Imaging data from 74 participants were analyzed, including individuals diagnosed with a schizophrenia-spectrum disorder ( $n = 31$ ) and nonpsychiatric healthy controls ( $n = 43$ ). There was no overlap in participant samples between the present study and our group's previous dEBC pilot study.<sup>49</sup> Within the clinical group (referred to as the schizophrenia group in this report), 21 participants were diagnosed with schizophrenia, 9 with schizoaffective disorder, and 1 with schizophreniform disorder. In the schizophrenia group, 81% of participants were prescribed antipsychotic medication at the time of study; chlorpromazine equivalents (CPZE)<sup>58</sup> were calculated. Healthy controls did not meet criteria for any of the assessed Axis I or II disorders or endorse any first-degree relatives with a psychotic disorder as assessed by the Family Interview for Genetic Studies.<sup>59</sup>

In addition to diagnostic interviews, the majority of participants completed neuropsychological testing, including the digit symbol coding test from the Wechsler Adult Intelligence Scale (WAIS-III)<sup>60</sup> and the letter

number sequencing test from the Wechsler Memory Scale (WMS-R).<sup>61</sup> Individuals in the schizophrenia group underwent assessment for psychotic symptoms with the Positive and Negative Psychotic Symptom Scale (PANSS).<sup>62</sup> Motor functioning was assessed in all participants using the International Cooperative Ataxia Rating Scale (ICARS).<sup>63</sup> The ICARS measures 19 cerebellar functions within the domains of posture and gait disturbances, kinetic functions, speech disorders, and oculomotor disorders.

#### Eyeblink Conditioning Procedure

Participants underwent single-cue delay eyeblink conditioning (dEBC) during fMRI scanning. Participants wore rubber laboratory goggles containing an infrared reflectance (IR) sensor lined up with the left pupil to measure blink activity and an attached tube to administer 50 ms air puffs (the US; 20 psi at the source) to the inner corner (toward the medial canthus) of the left eye. Participants also wore headphones through which they heard 400 ms 2 kHz auditory tones (the CS). During dEBC, neutral pictures from the International Affective Picture System<sup>64</sup> were presented in E-prime software, v2.0 (Psychology Software Tools, Pittsburgh, PA) that participants rated in terms of pleasantness with a response pad to maintain alertness. See prior reports for detailed information on a similar dEBC apparatus.<sup>49,65</sup>

Three consecutive 12 min scan sessions (referred to as “runs”) of dEBC were conducted (figure 1). Each run began and ended with a fixation period of 37.5 s in which participants were asked to keep their eyes focused on the white fixation cross centered on a black background. Each run contained 52 5 s trials with jittered intertrial

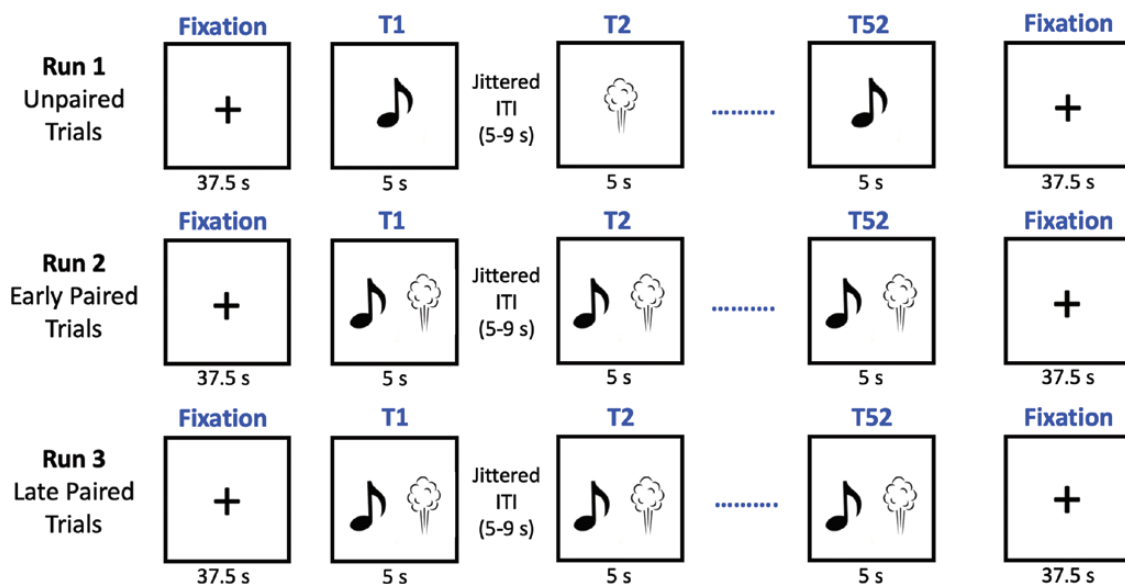


**Fig. 1.** Schematic of the delay eyeblink conditioning (dEBC) paradigm. Runs had 52 trials each. Each trial in run 1 contained either a tone or an air puff. Each trial in runs 2 and 3 contained a tone, which coterminated with an air puff. T, trial; ITI, intertrial interval.

intervals of 5–9 s. Run 1 consisted of 26 tones and 26 air puffs that were pseudorandomized with one event per trial. Runs 2 and 3 consisted of paired trials each containing a tone coterminating with an air puff. In paired trials, tone onset occurred 2 s into the trial, and air puffs were triggered at 2.32 s into the trial with a 29.5 ms delay to reach the eye after traveling through the tube. IR data were collected during the entire trial period at a rate of 1000 samples per second. Subsequently, run 1 of isolated tones and air puffs will be referred to as the “Unpaired Trials” phase, run 2 of paired trials as “Early Paired Trials,” and run 3 of paired trials as “Late Paired Trials.”

#### *Eyeblink Conditioning Data Processing*

Eyeblink IR data were processed using custom-made scripts in MATLAB (Release 2019a; The MathWorks, Inc., Natick, MA, USA). Data were segmented into 1086 ms epochs and grouped into 3 blocks (block 1: 26 US trials; blocks 2 and 3: each 52 paired CS-US trials) to align with the fMRI runs and maximize the number of trials. The 225 ms before CS onset was designated as the trial baseline (Supplementary Figure S1). Data underwent baseline normalization via mean subtraction and filtering with a moving average quadratic robust regression filter. Trials were excluded upon visual inspection due to blink activity occurring in the baseline period and/or poor IR signal (eg, signal railing, implausible physiological signals). In the remaining trials, alpha responses (ie, startle responses to auditory stimuli), CRs, and URs were all classified as IR activity exceeding 5 standard deviations (SDs) above baseline in the following time windows: alpha responses: 25–100 ms after CS onset; CRs: 100–350 ms after CS onset; UR: US onset until the end of the epoch. Peak CR and UR latencies were measured as the time point of maximal IR amplitude, with the timing relative to CS and US onsets, respectively. Planned behavioral analyses included repeated measures analyses of variance (ANOVAs) in SPSS (IBM SPSS Statistics for macOS, Version 27.0) with factors of diagnostic group and MRI run and dependent variables of percent CRs, CR peak latency, and UR peak latency. Given the sensitivity of the percent CRs metric to the amount of included trials, participants' percentage of CRs were analyzed if they had 75% or more average IR trials remaining after artifact rejection. A lower threshold at least one-third average remaining trials was imposed for the remaining IR indices to prioritize maximal data usage. Effect sizes reported are partial eta squared values.

#### *MRI Data Acquisition*

Whole brain functional and structural data were acquired on a 3T MRI system (Magnetom, TrioTim, Siemens) at Indiana University Bloomington, IN, USA. T1-weighted

anatomical scans were collected with a 32-channel coil and had the following parameters: repetition time (TR) 1800 ms, echo time (TE) 2.67 ms, flip angle (FA) = 9°, voxel size  $1 \times 1 \times 1 \text{ mm}^3$ ,  $256 \times 256$  image matrix, and 192 slices on the sagittal plane. Functional scans were collected with a 12-channel coil using an echo-planar imaging (EPI) sequence with interleaved acquisition and the following parameters: TR 2500 ms, TE 30 ms, FA 80°, voxel size  $2.3 \times 2.3 \times 3.2 \text{ mm}^3$ ,  $96 \times 96$  image matrix, 40 slices, and 280 volumes.

#### *MRI Preprocessing and SUIT Normalization*

MRI preprocessing was performed using SPM12 (<https://www.fil.ion.ucl.ac.uk/spm/software/spm12>) and the SUIT toolbox v3.4 (<http://www.diedrichsenlab.org/imaging/suit.htm>). Functional images underwent slice-timing correction, realignment to the run 1 mean image, and coregistration to the intensity bias-corrected anatomical image. Framewise displacement (FD, the amount of participant head movement at each EPI volume acquisition)<sup>66</sup> was calculated using 6 rigid-body motion parameters, and volumes with FD > 1 mm (including one preceding and two following the suprathreshold volume) were flagged as high motion volumes. The percentage of high motion scans across participants averaged over runs ranged from 0% to 21.67% scans ( $M = 2.78$ ,  $SD = 5.12$ ), with a higher percentage in the schizophrenia than control group ( $t = -2.3$ ,  $P = .026$ ). Therefore, these volumes were incorporated as regressors of no interest into each participant's design matrix. No participants were excluded due to excess motion. Scans were segmented into regions of grey matter, white matter, and cerebrospinal fluid and normalized to the Montreal Neurological Institute (MNI152) brain template for whole brain analysis and the SUIT cerebellum and brainstem template using SPM's Dartel function for cerebellar-specific analysis. Coregistered functional scans were transformed to standard space using the normalization parameters. After normalization, whole brain and cerebellar functional images were resliced with 2-mm isotropic voxels and spatially smoothed with 6-mm full-width half maximum (FWHM) Gaussian kernel.

#### *fMRI Analyses*

Neural activation during the eyeblink conditioning task was examined using the general linear model in preliminary whole brain analyses followed by cerebellar-specific SUIT analyses. The fMRI design matrix included fixation period onsets and durations, event-related unpaired and paired tone and air puff stimuli from runs 1–3, and motion regressors not convolved with the hemodynamic response (6 motion parameters, FD-based censored scans). Within- and between-groups *t*-test contrasts of interest were Early Paired Trials



– Unpaired Trials and Late Paired Trials – Unpaired Trials for cerebellar and whole brain analyses, as well as Unpaired Trials – Fixation for whole brain analysis to check for expected cortical activation related to auditory and somatosensory stimuli. Reverse contrasts were also examined.

The activation significance thresholds were computed with 3dFWHMx and 3dClustSim in AFNI (<https://afni.nimh.nih.gov>). Spatial autocorrelation functions (ACF) were computed for participants' first-level residuals, and 10 000 Monte Carlo simulations were run on the average ACF values. A voxel-wise  $P < .001$  for a corrected  $P < .05$  and 2-sided 1st-nearest neighbor clustering resulted in significance thresholds of  $k_E = 60$  voxels for whole brain analysis and  $k_E = 29$  voxels for SUIT analyses. The probabilistic SUIT atlas<sup>67</sup> was used to identify cerebellar lobules, and cerebellar activation was overlaid on the SUIT toolbox cerebellar flatmap<sup>68</sup> for visualization purposes.

For the subsequent ROI analysis using the MarsBaR toolbox (<http://marsbar.sourceforge.net>), average weights of each contrast of interest (Early Paired Trials – Unpaired Trials and Late Paired Trials – Unpaired Trials) were extracted from the hypothesized regions related to dEBC functioning (lobule VI) and higher-order cognitive processes (Crus I). ROIs were defined as whole cerebellar lobules from the Automatic Anatomical Labeling Atlas<sup>69</sup> using the WFU PickAtlas tool v3.0.5.<sup>70</sup> Preliminary analyses showed high correlation of cerebellar activation in the left and right hemisphere ( $r > .91$  for lobule VI contrasts and  $r > .86$  for Crus I contrasts). Weights for bilateral lobular activations were therefore averaged to increase statistical power and reduce the number of comparisons for subsequent analysis, resulting in four bilateral ROIs. Independent samples  $t$ -tests were then conducted between schizophrenia and control groups for each region and contrast, with the significance level set

at  $P < .05$  for these tests and the following correlational analyses.

### Cerebellar Activation Correlations with Cognitive and Symptom Measures

In the full sample, exploratory bivariate Pearson correlation was calculated between mean cerebellar activation from the ROI masks, letter number sequencing scaled scores as an index of working memory capacity, and digit symbol scaled scores as an index of processing speed. In the schizophrenia group, cerebellar activation was correlated with PANSS positive and negative symptom subscale scores. PANSS positive scores were positively skewed and were thus log-transformed.

## Results

### Sample Characteristics and Eyeblink Conditioning Results

Healthy control and schizophrenia groups did not significantly differ in age or sex but did differ in racial/ethnic identification (Table 1). On average, participants in the schizophrenia group compared to controls had lower letter number sequencing and digit symbol scores and higher ICARS cerebellar ataxia scores.

IR data from 6 participants (3 healthy controls [HC]; 3 participants in the schizophrenia group [SZ]) were excluded from initial behavioral processing due to low signal quality. In the remaining 68 participants, the healthy control group had significantly more remaining trials ( $M = 72.95\%$ ;  $SD = 16.17\%$ ) than the schizophrenia group ( $M = 55.82\%$ ,  $SD = 17.95\%$ ) after trial rejections due to IR signal noise and/or blinks in the baseline period ( $P < .001$ ). Alpha responses in paired trial runs were infrequent ( $M = 2.15$ ;  $SD = 2$ ) and did not significantly differ between groups. Analysis of percent CRs in participants with  $>75\%$  trials showed a significant increase in percent CRs

**Table 1.** Sample Characteristics

	Healthy Control Group	Schizophrenia Group	Statistics
<i>n</i>	43	31	–
Age	39.02 (9.91)	36.81 (11.45)	$t(72) = 0.89$
Sex (female/male)	23/20	11/20	$\chi^2(1) = 2.35$
Race or ethnicity (C/B/H/M)	35/6/0/2	14/13/1/1 <sup>b</sup>	$\chi^2(3) = 10.59^*$
LN sequencing	11.83 (2.44) <sup>b</sup>	9.52 (2.21) <sup>b</sup>	$t(68) = 4.06^{***}$
Digit symbol coding	12.4 (2.94)	7.6 (2.31) <sup>a</sup>	$t(71) = 7.47^{***}$
ICARS	0.77 (1.36)	3.73 (4.08) <sup>a</sup>	$t(33.54) = -3.84^{**}$
PANSS positive	–	14 (6.07) <sup>b</sup>	–
PANSS negative	–	12.83 (4.29) <sup>b</sup>	–

*Note:* Values represent frequencies for sex and race/ethnicity and mean (standard deviation) for the remaining variables. C, Caucasian; B, Black or African American; H, Hispanic or Latino; M, Multiracial; LN sequencing, letter number sequencing; ICARS, International Cooperative Ataxia Rating Scale; PANSS, Positive and Negative Syndrome Scale.

<sup>a</sup>Missing data from 1 participant.  
<sup>b</sup>Missing data from 2 participants.  
 $*P < .05$ ;  $**P < .01$ ;  $***P < .001$ .

over runs (HC  $n = 24$ ; SZ  $n = 5$ ;  $F(2,56) = 14.19$ ,  $P < .001$ ,  $\eta_p^2 = 0.34$ ) (Supplementary Figure S2). Diagnostic differences in percent CRs could not be reliably examined due to insufficient remaining trials in the schizophrenia group. Analysis of response timing in participants with at least one-third usable trials showed significantly longer CR peak latencies across runs (HC  $n = 34$ ; SZ  $n = 22$ ;  $F(1.7,90.5) = 4.26$ ,  $P = .023$ , Greenhouse–Geisser corrected,  $\eta_p^2 = .07$ ). Diagnostic group and group-by-run interaction effects for CR peak latencies were not significant. URs (eyeblinks to the air puff) reliably occurred for both groups for trials in all three runs (~99% in participants with at least one-third usable trials) and were visibly apparent even in participants' excluded trials. Analyses showed significantly shorter UR peak latencies over time (HC  $n = 39$ ; SZ  $n = 24$ ;  $F(1.4,87.3) = 4.19$ ,  $P = .03$ , Greenhouse–Geisser corrected,  $\eta_p^2 = 0.06$ ), with no significant group effect or group-by-run interaction. Using Spearman's rho, antipsychotic dosage (CPZE) did not significantly correlate with CR peak latency (all runs  $\rho < |0.14|$ ,  $P > .5$ ) or UR peak latency during paired trials ( $\rho < |0.22|$ ,  $P > .3$ ), but CPZE did positively correlate with UR peak latency during unpaired trials ( $\rho = 0.44$ ,  $P = .048$ ).

### fMRI Results

Preliminary whole brain analyses revealed robust activation to unpaired trials compared to fixation in bilateral temporal and parietal areas in healthy control and schizophrenia groups, with greater activation in the schizophrenia than control group in the middle cingulate cortex (figure 2). Early paired trials and late paired trials compared to unpaired trials contrasts revealed widespread bilateral activation in the healthy control group in posterior cerebellar (eg, lobule VI, Crus I–II),

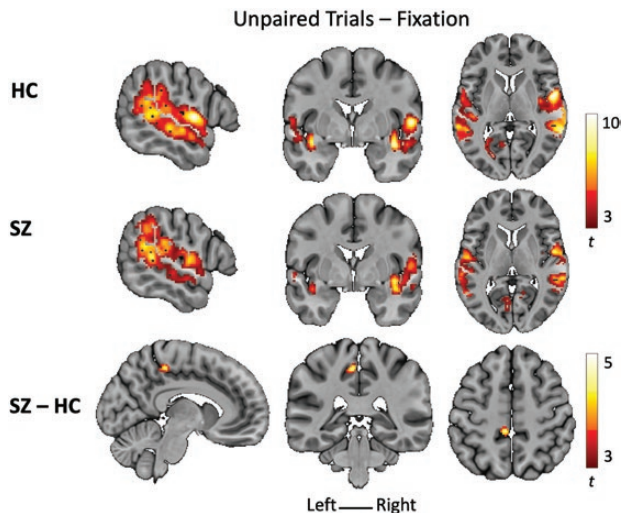


**Fig. 2.** Whole brain activation in the healthy control (HC) and schizophrenia (SZ) groups during unpaired air puff and tone trials compared to fixation periods, significant at a threshold of voxel-wise  $P < .001$  and  $k_E = 60$  for a corrected  $P < .05$ .

thalamic, parietal, temporal, frontal, occipital, and cingulate regions (Supplementary Material). The schizophrenia group exhibited less significant activation in these contrasts, confined to the left superior temporal gyrus (early conditioning) and the right inferior occipital gyrus and right inferior parietal lobule (late conditioning). Controls showed greater activation than the schizophrenia group during paired trials peaking in the precuneus (early conditioning), as well as the angular/supramarginal gyrus and calcarine gyrus (late conditioning). See Supplementary Material for whole brain activation tables and figures.

In the cerebellar SUIT analyses, one-sample  $t$ -tests of conditioning contrasts in the healthy control group revealed multiple significant clusters of cerebellar activation (figure 3; Table 2). During early paired trials compared to unpaired trials, the strongest activation cluster peaked in right hemispheric lobule VI. Additional significant clusters peaked in left lobule VI, right hemispheric and vermis lobule VIIIb, right Crus II, and the brain stem. During late paired trials compared to unpaired trials in healthy controls, the strongest activation cluster peaked in left lobule VI, and two larger clusters peaked in right Crus I and right lobule VI. In the schizophrenia group, significant cerebellar activation was not detected in early nor late paired trials compared to unpaired trials, yet cerebellar activation did not significantly differ between groups in a two-sample  $t$ -test. Of note, clusters below the significance threshold suggested a pattern of greater activation in the control than the schizophrenia group peaking in left lobule VI ( $k_E = 24$ ,  $t = 4.5$ , MNI =  $-34, -46, -35$ ) and the brain stem ( $k_E = 23$ ,  $t = 4.29$ , MNI =  $16, -24, -7$ ) for early paired trials compared to unpaired trials and peaking in left Crus I ( $k_E = 16$ ,  $t = 4.36$ , MNI =  $-36, -44, -37$ ) for late paired trials compared to unpaired trials. No cerebellar regions showed significantly greater activation during unpaired trials compared to paired trials for either diagnostic group.

In the posterior cerebellar ROI analysis, healthy controls had higher Crus I activation than participants with schizophrenia during late paired trials compared to unpaired trials (figure 4; Supplementary Table S4). Group differences were not significant for Crus I in the Early Paired Trials – Unpaired Trials contrast or lobule VI in either contrast. Exploratory post hoc paired  $t$ -tests within each diagnostic group showed that healthy controls had significantly greater right compared to left Crus I activation in the late conditioning contrast ( $t(42) = -3.1$ ,  $P = .003$ ); there were no other significant hemispheric differences in ROI activation.

Using Spearman's rho, antipsychotic dosage (CPZE) in the schizophrenia group did not significantly correlate with lobule VI or Crus I activation for early or late conditioning contrasts ( $\rho < |0.14|$ ,  $P > .4$ ). Next, follow-up independent samples  $t$ -tests were run separately for healthy control and schizophrenia groups to determine whether similar activation magnitudes were evident in participants included and

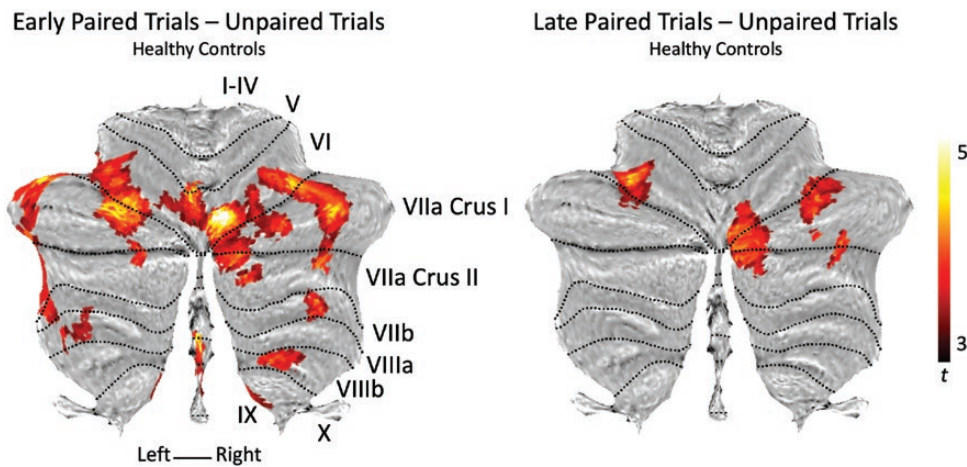


**Fig. 3.** Cerebellar activation in healthy controls overlaid on the SUIT flat surface map, significant at a threshold of voxel-wise  $P < .001$  and  $k_E = 29$  voxels for a corrected  $P < .05$ . No cerebellar activation reached significance in the schizophrenia group.

**Table 2.** Cerebellar Activation in Healthy Controls During Eyeblink Conditioning

Contrast	Coordinates (mm)	Cluster Size (mm <sup>3</sup> )	t	Region	Side
Early paired trials – unpaired trials	10 -74 -17	809	6.29	Lobule VI, extending into Lobule VIIa Crus I	R
	-34 -44 -33	154	4.68	Lobule VI	L
	0 -64 -43	32	4.61	Lobule VIIIb vermis	-
	36 -58 -45	40	4.49	Lobule VIIa Crus II	R
	16 -58 -53	52	4.34	Lobule VIIIb	R
	18 -86 -37	32	4.22	Lobule VIIa Crus II	R
Late paired trials – unpaired trials	16 -26 -1	43	4.06	Brain stem	R
	-32 -58 -25	88	4.84	Lobule VI	L
	32 -68 -31	152	4.75	Lobule VIIa Crus I	R
	12 -74 -25	155	4.43	Lobule VI, Lobule VIIa Crus I	R

*Note:* Significant activation from cerebellar-specific SUIT analyses in the healthy control group ( $n = 43$ ). Voxel-wise threshold of  $P < .001$  and  $k_E = 29$  voxels for a corrected  $P < .05$  (height threshold:  $t = 3.3$ ). Peak voxel coordinates are in MNI space. R, right hemisphere; L, left hemisphere. No cerebellar activation reached significance in the schizophrenia group.

excluded from the IR behavioral analyses. There were no significant differences in lobule VI or Crus I activation in the early or late conditioning contrasts for participants included vs. excluded from the percent CRs or CR peak latency analyses ( $P > .05$ ).

#### *Cerebellar Activation Correlations with Cognitive and Symptom Measures*

In the full sample, letter number sequencing scaled scores positively correlated with lobule VI and Crus I activation in the Late Paired Trials – Unpaired Trials contrast (figure 5; Supplementary Table S5). Log-transformed PANSS positive scores were inversely correlated with Crus I activation in the Late Paired Trials – Unpaired Trials contrast and showed a similar yet nonsignificant pattern in lobule VI. Exploratory post hoc analyses showed that these significant correlations showed the same patterns for both left and right hemispheres. Remaining correlations were not significant.

#### **Discussion**

The present work is the largest fMRI study to date to examine neural correlates of delay eyeblink conditioning (dEBC) in individuals with schizophrenia-spectrum disorders utilizing cerebellar-specific processing methods. These novel findings illustrate relationships between cerebellar function during dEBC, psychotic symptoms, and cognition, extending our understanding of the role of the cerebellum in psychosis and supporting the cognitive dysmetria framework. To summarize, analyses revealed cerebellar activation during dEBC in healthy controls in key regions of the associative learning circuit such as posterior lobule VI and a lack of significant activation in the schizophrenia group. ROI analyses revealed lower activation in the schizophrenia group than controls in Crus I, a region involved in higher-order cognitive processes.<sup>51,71,72</sup> Moreover, greater Crus I activation was correlated with higher verbal working memory capacity across the full sample and lower positive psychotic symptom severity in the schizophrenia group. These findings indicate



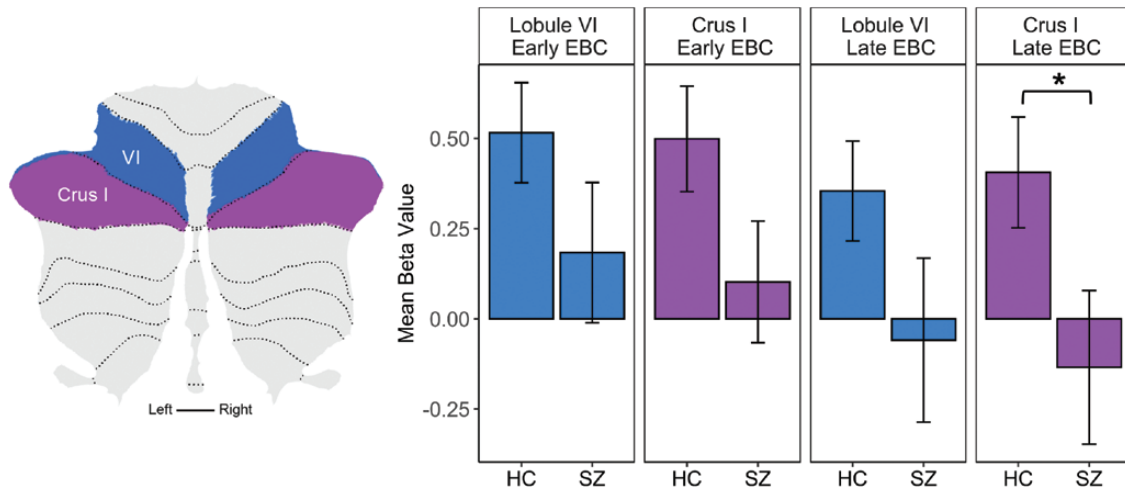


**Fig. 4.** Cerebellar region of interest (ROI) analysis. *Left:* Images of left and right hemisphere lobule VI and Crus I ROI masks overlaid on the SUI flat surface map. *Right:* Mean beta values from healthy control (HC) and schizophrenia (SZ) groups from each averaged bilateral ROI for Early Paired Trials – Unpaired Trials (Early EBC) and Late Paired Trials – Unpaired Trials (Late EBC) contrasts. Error bars represent  $\pm 1$  standard error of the mean.  $*P < .05$ .

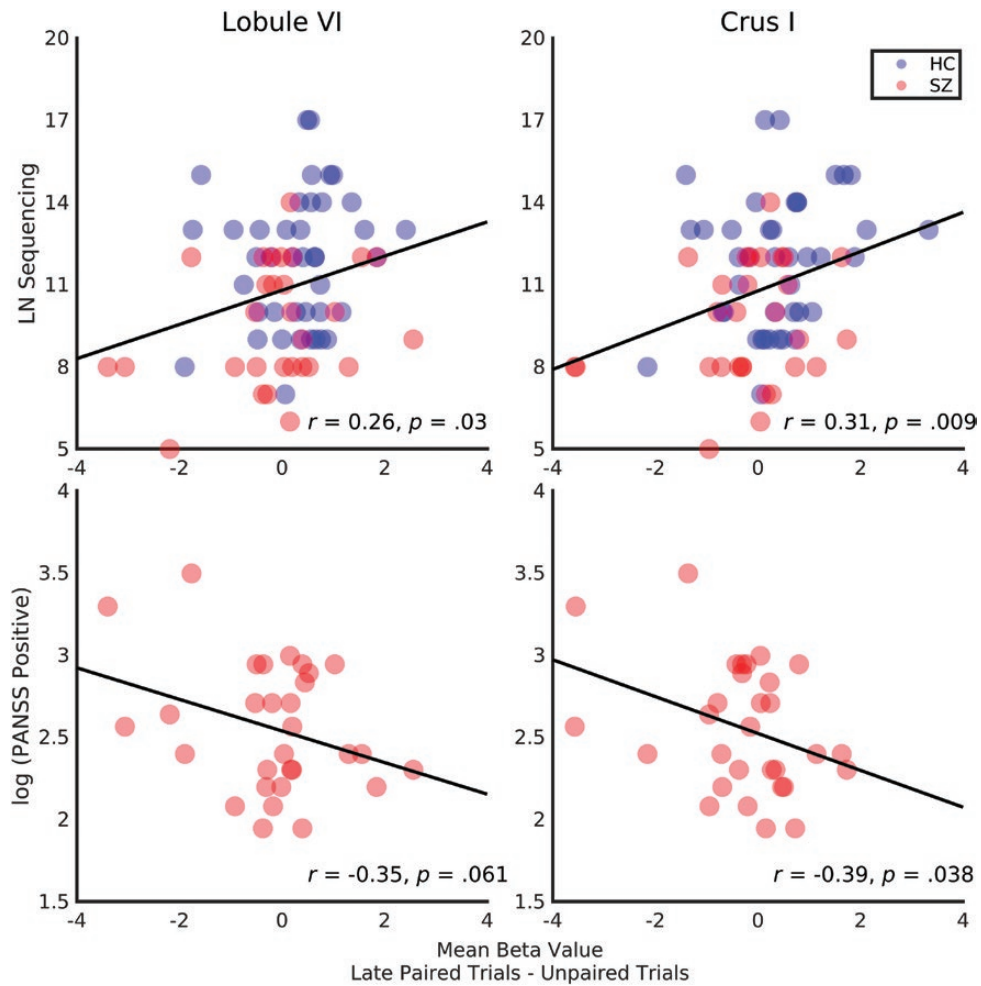


**Fig. 5.** Scatter plots of bilateral lobule VI and Crus I activation in the Late Paired Trials – Unpaired Trials contrast in the healthy control (HC) and schizophrenia (SZ) groups. *Top:* Activation related to letter number (LN) sequencing scaled scores in the full participant sample. *Bottom:* Activation related to log-transformed Positive and Negative Syndrome Scale (PANSS) positive subscale scores in the schizophrenia group.



that reported deficits in basic associative learning processes in schizophrenia<sup>27,35</sup> may be related to disruptions recruiting regions of the posterior cerebellum which also contribute to coordination of cognitive processes and predictive coding.<sup>73-77</sup>

Cerebellar regions activated during dEBC in healthy control participants largely aligned with prior literature, particularly posterior lobules VI and Crus I-II during both phases of dEBC and lobule VIIIb during early phase dEBC.<sup>44-48</sup> Of note, the deep cerebellar nuclei have been identified as critical for the formation and storage of the essential dEBC memory trace in nonhuman animal literature,<sup>37,38</sup> yet they were not significantly activated in the present analyses. Prior human studies using 7T MRI have identified activation of the cerebellar deep nuclei during dEBC<sup>46,48</sup> more often than studies using 3T MRI such as the current study. Regarding hemispheric laterality, lesion studies in nonhuman animals have typically implicated cerebellar regions ipsilateral to the eye receiving the unconditioned stimulus in dEBC.<sup>36</sup> However, neuroimaging studies in humans<sup>31,45,46</sup> as well as rabbits<sup>78</sup> have found dEBC to activate a bilateral network of cerebellar regions including lobule VI, aligning with the present findings. Finally, while the cerebellum was the focus of this and many other dEBC studies, widespread conditioning-related activation in the cerebral cortex was detected in the healthy control group as in prior reports,<sup>79-82</sup> suggesting that a broader neural circuit is recruited in conjunction with cerebellar regions during this form of associative learning.

Individuals with schizophrenia-spectrum disorders showed diminished cerebellar activation during the dEBC task, aligning with our pilot study.<sup>49</sup> In preliminary whole brain and SUIT analyses, no cerebellar activation passed the cluster correction threshold for early or late conditioning contrasts for the schizophrenia group. In clusters below our significance threshold, activation in left lobule VI (early dEBC) and Crus I (late dEBC) trended toward previous PET findings of reduced ipsilateral activation during dEBC acquisition in schizophrenia compared to controls.<sup>31</sup> ROI analyses of lobule VI and Crus I revealed a pattern of lower activation in the schizophrenia group than controls, with a significant difference in Crus I during late dEBC. Interestingly, the average beta weights during the late phase of dEBC were negative in the schizophrenia group, indicating slightly higher activation to unpaired than paired stimuli. Moreover, whole brain analyses revealed that the schizophrenia group showed robust temporal, motor, and cingulate activation to the unpaired stimuli that was greater in the middle cingulate cortex than activation in healthy controls, but diminished conditioning-related activation in cerebellar and cortical regions. While speculative, this pattern of results may suggest a disruption in the dEBC neural circuitry in psychotic illness in which the posterior cerebellum's

temporal prediction and modeling mechanisms as well as communication with cerebral regions are impaired, thus diminishing precisely timed associations between conditioned and unconditioned stimuli. Further studies are needed to establish whether this altered neural activation relates to behavioral dEBC deficits, as group differences in conditioning rates could not be reliably analyzed, and timing results suggested adaptively timed peak latencies in both groups (ie, peak conditioned response latencies occurring closer to the air puff in late compared to early paired trials).<sup>28</sup>

The finding of lower Crus I activation during late dEBC in individuals with schizophrenia compared to controls is of particular interest given the region's involvement in higher-order cognitive processes. Studies have found posterior cerebellar Crus I to have structural and functional connectivity to the prefrontal cortex that is distinct from circuitry of the anterior cerebellum to motor cortices.<sup>83-85</sup> Neuroimaging studies have also identified Crus I as a region that is preferentially activated during cognitive and language-based tasks such as working memory and verb generation.<sup>51</sup> Therefore, present findings of diminished Crus I activation during dEBC in schizophrenia in conjunction with the positive correlation between Crus I activation and working memory capacity may suggest a relationship between aberrant associative learning and higher-order cognitive deficits seen in psychosis. Lobule VI activation was also positively correlated with working memory capacity, aligning with work showing greater lobule VI activation with increased working memory load.<sup>52,53</sup> Finally, diminished Crus I activation during late dEBC correlated with higher positive psychotic symptom severity. We interpret this finding to indicate that impaired neural function as measured during associative learning may relate to increased prediction errors and misattribution of salience to irrelevant stimuli,<sup>77</sup> thus increasing the likelihood of hallucinations and delusions. However, the average symptom load in the present sample was relatively low (perhaps in part due to the intensive nature of the study resulting in a higher functioning sample), and this correlation may have been driven by a few individuals with high symptom severity. Future studies with a wider severity range should examine whether more pronounced reductions in cerebellar activity emerge with more severe loading of positive symptoms.

This study had several limitations. First, the suboptimal quality of the infrared reflectance (IR) data limits the interpretation of the fMRI findings, as the high variability in cerebellar activations may largely relate to individual differences in conditioning rates. While IR signal is useful in its MRI compatibility, it is an indirect measure of dEBC activity based on light reflectance during eyelid closure. In behavioral studies, electromyography (EMG) is the gold standard for measuring dEBC as it directly indexes the propensity to blink via acute measurement of contractions of the orbicularis muscle, thus yielding information closer to the behavioral response. It is also possible that the goggles occasionally shifting while participants were lying

in the scanner led to less reliable signal than IR markers attached directly to the participants' eyelids.<sup>46,48</sup> However, while the inability to reliably measure diagnostic group differences in percent conditioned responses limits the interpretation of the diminished cerebellar activation found in the schizophrenia group, other data in this sample suggest motor and timing impairments in these participants. For example, motor abnormalities as measured by the ICARS were greater in the schizophrenia group compared to controls. Additionally, most of the present sample underwent a sensorimotor synchronization task during fMRI in our group's previously published report.<sup>11</sup> Findings demonstrated alterations in the schizophrenia group compared to controls in the timing and force of self-paced finger tapping as well as effective cerebellar connectivity with the primary motor cortex and thalamus (64% of the present dEBC sample was included in behavioral analyses and 85% in the imaging analyses of this prior study).

Another limitation of the present study relates to recent research suggesting that the topography of task-related cerebellar activations may not respect traditionally defined lobular boundaries.<sup>86</sup> Therefore, future studies should investigate whether functionally defined parcellations better capture dEBC-related neural activity. Finally, future 7T MRI studies hold promise for examining whether deep cerebellar nuclei activation is altered during dEBC in schizophrenia.

Overall, these novel findings extend our understanding of neural circuitry that has been implicated in prior reports of delay eyeblink conditioning in schizophrenia and lend support to the cognitive dysmetria framework, which posits a discoordination between associative threads rooted in aberrant cerebellar function. Future studies in individuals with psychotic-spectrum disorders are warranted to further elucidate the relationship between associative learning, cognitive deficits, and cortico-cerebellar-thalamic-cortical circuit function.

### Supplementary Material

Supplementary data are available at *Schizophrenia Bulletin Open* online.

### Funding

This work was supported by the National Institute of Mental Health (R01 MH074983 to W.P.H.; R21 MH091774 to B.F.O.; T32 MH103213 to W.P.H., N.B.L., A.B.M., and J.R.P.; F31 MH119767 to A.B.M.; F31 MH122122 to J.R.P.), the National Science Foundation Graduate Research Fellowship Program (1342962 to N.B.L.), the Indiana Clinical and Translational Sciences Institute Award (TL1 TR001107 and UL1 TR001108 to A.B.M. and J.R.P.), and the Brain and Behavior Research Foundation (NARSAD Young Investigator Award to A.R.B.). This research was also supported in part by Lilly Endowment, Inc. through its support for the Indiana

University Pervasive Technology Institute, which provided supercomputing resources that contributed to this research (<https://pti.iu.edu/>).

### Acknowledgments

We would like to thank the participants and their families for participation in this study. We also thank Patricia Sparks and Lisa Bartolomeo for coordinating and running study visits, the IUB Imaging Research Facility staff, and the Psychological and Brain Sciences technical support group including Jeff Sturgeon. The authors have declared that there are no conflicts of interest in relation to the subject of this study.

### References

1. Andreasen NC, Paradiso S, O'Leary DS. "Cognitive dysmetria" as an integrative theory of schizophrenia: a dysfunction in cortical-subcortical-cerebellar circuitry? *Schizophr Bull.* 1998;24:203–218.
2. Chua SE, Cheung C, Cheung V, et al. Cerebral grey, white matter and csf in never-medicated, first-episode schizophrenia. *Schizophr Res.* 2007;89:12–21.
3. Kühn S, Romanowski A, Schubert F, Gallinat J. Reduction of cerebellar grey matter in Crus I and II in schizophrenia. *Brain Struct Funct.* 2012;217:523–529.
4. McDonald C, Bullmore E, Sham P, et al. Regional volume deviations of brain structure in schizophrenia and psychotic bipolar disorder: computational morphometry study. *Br J Psychiatry* 2005;186:369–377.
5. Kim DJ, Kent JS, Bolbecker AR, et al. Disrupted modular architecture of cerebellum in schizophrenia: a graph theoretic analysis. *Schizophr Bull.* 2014;40:1216–1226.
6. Koch K, Wagner G, Dahnke R, et al. Disrupted white matter integrity of corticopontine-cerebellar circuitry in schizophrenia. *Eur Arch Psychiatry Clin Neurosci.* 2010;260:419–426.
7. Okugawa G, Nobuhara K, Minami T, et al. Neural disorganization in the superior cerebellar peduncle and cognitive abnormality in patients with schizophrenia: a diffusion tensor imaging study. *Prog Neuropsychopharmacol Biol Psychiatry* 2006;30:1408–1412.
8. Tanskanen P, Ridler K, Murray GK, et al. Morphometric brain abnormalities in schizophrenia in a population-based sample: relationship to duration of illness. *Schizophr Bull.* 2010;36:766–777.
9. Bernard JA, Mittal VA. Dysfunctional activation of the cerebellum in schizophrenia: a functional neuroimaging meta-analysis. *Clin Psychol Sci.* 2015;3:545–566.
10. Li Z, Huang J, Hung KSY, et al. Cerebellar hypoactivation is associated with impaired sensory integration in schizophrenia. *J Abnorm Psychol.* 2021;130:102–111.
11. Moussa-Tooks AB, Kim DJ, Bartolomeo LA, et al. Impaired effective connectivity during a cerebellar-mediated sensorimotor synchronization task in schizophrenia. *Schizophr Bull.* 2019;45:531–541.
12. Bernard JA, Dean DJ, Kent JS, et al. Cerebellar networks in individuals at ultra high-risk of psychosis: impact on postural sway and symptom severity. *Hum Brain Mapp.* 2014;35:4064–4078.
13. Clark SV, Tannahill A, Calhoun VD, Bernard JA, Bustillo J, Turner JA. Weaker cerebello-cortical connectivity within

- sensorimotor and executive networks in schizophrenia compared to healthy controls: relationships with processing speed. *Brain Connect.* 2020;10:490–503.
14. Kim DJ, Moussa-Tooks AB, Bolbecker AR, *et al.* Cerebellar-cortical dysconnectivity in resting-state associated with sensorimotor tasks in schizophrenia. *Hum Brain Mapp.* 2020;41:3119–3132.
  15. Shinn AK, Baker JT, Lewandowski KE, Öngür D, Cohen BM. Aberrant cerebellar connectivity in motor and association networks in schizophrenia. *Front Hum Neurosci.* 2015;9:134.
  16. Wang L, Zou F, Shao Y, *et al.* Disruptive changes of cerebellar functional connectivity with the default mode network in schizophrenia. *Schizophr Res.* 2014;160:67–72.
  17. Kent JS, Hong SL, Bolbecker AR, *et al.* Motor deficits in schizophrenia quantified by nonlinear analysis of postural sway. *PLoS One.* 2012;7:e41808.
  18. Marvel CL, Schwartz BL, Rosse RB. A quantitative measure of postural sway deficits in schizophrenia. *Schizophr Res.* 2004;68:363–372.
  19. Carroll CA, O'Donnell BF, Shekhar A, Hetrick WP. Timing dysfunctions in schizophrenia as measured by a repetitive finger tapping task. *Brain Cogn.* 2009;71:345–353.
  20. Bartolomeo LA, Shin Y-W, Block HJ, *et al.* Prism Adaptation Deficits in Schizophrenia. *Schizophr Bull.* 2020;46:1202–1209.
  21. Bigelow NO, Turner BM, Andreasen NC, Paulsen JS, O'Leary DS, Ho BC. Prism adaptation in schizophrenia. *Brain Cogn.* 2006;61:235–242.
  22. Carroll CA, Boggs J, O'Donnell BF, Shekhar A, Hetrick WP. Temporal processing dysfunction in schizophrenia. *Brain Cogn.* 2008;67:150–161.
  23. Elvevåg B, McCormack T, Gilbert A, Brown GD, Weinberger DR, Goldberg TE. Duration judgements in patients with schizophrenia. *Psychol Med.* 2003;33:1249–1261.
  24. Lee KH, Bhaker RS, Mysore A, Parks RW, Birkett PB, Woodruff PW. Time perception and its neuropsychological correlates in patients with schizophrenia and in healthy volunteers. *Psychiatry Res.* 2009;166:174–183.
  25. Damme KSF, Gallagher N, Vargas T, Osborne KJ, Gupta T, Mittal VA. Motor sequence learning and pattern recognition in youth at clinical high-risk for psychosis. *Schizophr Res.* 2019;208:454–456.
  26. Green MF, Kern RS, Williams O, McGurk S, Kee K. Procedural learning in schizophrenia: evidence from serial reaction time. *Cogn Neuropsychiatry* 1997;2:123–134.
  27. Kent JS, Bolbecker AR, O'Donnell BF, Hetrick WP. Eyeblink conditioning in schizophrenia: a critical review. *Front Psychiatry* 2015;6:146.
  28. Bolbecker AR, Mehta CS, Edwards CR, Steinmetz JE, O'Donnell BF, Hetrick WP. Eye-blink conditioning deficits indicate temporal processing abnormalities in schizophrenia. *Schizophr Res.* 2009;111:182–191.
  29. Brown SM, Kieffaber PD, Carroll CA, *et al.* Eyeblink conditioning deficits indicate timing and cerebellar abnormalities in schizophrenia. *Brain Cogn.* 2005;58:94–108.
  30. Hofer E, Doby D, Anderer P, Dantendorfer K. Impaired conditional discrimination learning in schizophrenia. *Schizophr Res.* 2001;51:127–136.
  31. Parker KL, Andreasen NC, Liu D, Freeman JH, O'Leary DS. Eyeblink conditioning in unmedicated schizophrenia patients: a positron emission tomography study. *Psychiatry Res.* 2013;214:402–409.
  32. Sears LL, Andreasen NC, O'Leary DS. Cerebellar functional abnormalities in schizophrenia are suggested by classical eyeblink conditioning. *Biol Psychiatry* 2000;48:204–209.
  33. Forsyth JK, Bolbecker AR, Mehta CS, *et al.* Cerebellar-dependent eyeblink conditioning deficits in schizophrenia spectrum disorders. *Schizophr Bull.* 2012;38:751–759.
  34. Bolbecker AR, Kent JS, Petersen IT, *et al.* Impaired cerebellar-dependent eyeblink conditioning in first-degree relatives of individuals with schizophrenia. *Schizophr Bull.* 2014;40:1001–1010.
  35. Reeb-Sutherland BC, Fox NA. Eyeblink conditioning: a non-invasive biomarker for neurodevelopmental disorders. *J Autism Dev Disord.* 2015;45:376–394.
  36. Thompson RF, Steinmetz JE. The role of the cerebellum in classical conditioning of discrete behavioral responses. *Neuroscience* 2009;162:732–755.
  37. Christian KM, Thompson RF. Long-term storage of an associative memory trace in the cerebellum. *Behav Neurosci.* 2005;119:526–537.
  38. McCormick DA, Thompson RF. Cerebellum: essential involvement in the classically conditioned eyelid response. *Science* 1984;223:296–299.
  39. Steinmetz JE, Sengelaub DR. Possible conditioned stimulus pathway for classical eyelid conditioning in rabbits. I. Anatomical evidence for direct projections from the pontine nuclei to the cerebellar interpositus nucleus. *Behav Neural Biol.* 1992;57:103–115.
  40. Schreurs BG, Sanchez-Andres JV, Alkon DL. Learning-specific differences in Purkinje-cell dendrites of lobule HVI (Lobulus simplex): intracellular recording in a rabbit cerebellar slice. *Brain Res.* 1991;548:18–22.
  41. Lavond DG, Steinmetz JE, Yokaitis MH, Thompson RF. Reacquisition of classical conditioning after removal of cerebellar cortex. *Exp Brain Res.* 1987;67:569–593.
  42. Yeo CH, Hardiman MJ, Glickstein M. Classical conditioning of the nictitating membrane response of the rabbit. II. Lesions of the cerebellar cortex. *Exp Brain Res.* 1985;60:99–113.
  43. Lavond DG, Steinmetz JE. Acquisition of classical conditioning without cerebellar cortex. *Behav Brain Res.* 1989;33:113–164.
  44. Cheng DT, Disterhoft JF, Power JM, Ellis DA, Desmond JE. Neural substrates underlying human delay and trace eyeblink conditioning. *Proc Natl Acad Sci U S A* 2008;105:8108–8113.
  45. Cheng DT, Meintjes EM, Stanton ME, *et al.* Functional MRI of cerebellar activity during eyeblink classical conditioning in children and adults. *Hum Brain Mapp.* 2014;35:1390–1403.
  46. Ernst TM, Thürling M, Müller S, *et al.* Modulation of 7 T fMRI signal in the cerebellar cortex and nuclei during acquisition, extinction, and reacquisition of conditioned eyeblink responses. *Hum Brain Mapp.* 2017;38:3957–3974.
  47. Ramnani N, Toni I, Josephs O, Ashburner J, Passingham RE. Learning- and expectation-related changes in the human brain during motor learning. *J Neurophysiol.* 2000;84:3026–3035.
  48. Thürling M, Kahl F, Maderwald S, *et al.* Cerebellar cortex and cerebellar nuclei are concomitantly activated during eyeblink conditioning: a 7T fMRI study in humans. *J Neurosci.* 2015;35:1228–1239.
  49. Kent JS, Kim DJ, Newman SD, Bolbecker AR, O'Donnell BF, Hetrick WP. Investigating cerebellar neural function in schizophrenia using delay eyeblink conditioning: a pilot fMRI study. *Psychiatry Res Neuroimaging* 2020;304:111133.
  50. Diedrichsen J. A spatially unbiased atlas template of the human cerebellum. *Neuroimage* 2006;33:127–138.



51. Stoodley CJ, Valera EM, Schmahmann JD. Functional topography of the cerebellum for motor and cognitive tasks: an fMRI study. *Neuroimage* 2012;59:1560–1570.
52. Chen SH, Desmond JE. Cerebrocerebellar networks during articulatory rehearsal and verbal working memory tasks. *Neuroimage* 2005;24:332–338.
53. Desmond JE, Gabrieli JD, Wagner AD, Ginier BL, Glover GH. Lobular patterns of cerebellar activation in verbal working-memory and finger-tapping tasks as revealed by functional MRI. *J Neurosci*. 1997;17:9675–9685.
54. First MB, Spitzer RL, Gibbon M, Williams JBW. *Structured Clinical Interview for DSM-IV-TR Axis I Disorders, Research Version, Patient Edition (SCID-I/P)*. New York: Biometrics Research; 2002.
55. First MB, Spitzer RL, Gibbon M, Williams JBW. *Structured Clinical Interview for DSM-IV-TR Axis I Disorders, Research Version, Non-Patient Edition (SCID-I/NP)*. New York: Biometrics Research; 2002.
56. First MB, Gibbon M, Spitzer RL, Williams JBW, Benjamin LS. *Structured Clinical Interview for DSM-IV Axis II Personality Disorders (SCID-II)*. Washington, DC: American Psychiatric Press, Inc.; 1997.
57. Sheehan DV, Lecrubier Y, Sheehan KH, et al. The Mini-International Neuropsychiatric Interview (M.I.N.I.): the development and validation of a structured diagnostic psychiatric interview for DSM-IV and ICD-10. *J Clin Psychiatry* 1998;59 Suppl 20:22–33;quiz 34–57.
58. Andreasen NC, Pressler M, Nopoulos P, Miller D, Ho BC. Antipsychotic dose equivalents and dose-years: a standardized method for comparing exposure to different drugs. *Biol Psychiatry* 2010;67:255–262.
59. Maxwell ME. *Family Interview for Genetics Studies (FIGS): A Manual for FIGS*. Bethesda, MD: Clinical Neurogenetics Branch, Intramural Research Program, National Institute of Mental Health Bethesda, MD; 1992.
60. Wechsler D. *WAIS III Administration and Scoring*. The San Antonio, TX: Psychological Corporation; 1997.
61. Wechsler D. *The Wechsler Memory Scale-Revised*. The San Antonio, TX: Psychological Corporation; 1987.
62. Kay SR, Fiszbein A, Opler LA. The positive and negative syndrome scale (PANSS) for schizophrenia. *Schizophr Bull*. 1987;13:261–276.
63. Trouillas P, Takayanagi T, Hallett M, et al. International Cooperative Ataxia Rating Scale for pharmacological assessment of the cerebellar syndrome. The Ataxia Neuropharmacology Committee of the World Federation of Neurology. *J Neurol Sci*. 1997;145:205–211.
64. Lang PJ, Bradley MM, Cuthbert BN. *The International Affective Picture System*. Gainesville, FL: Center for Research in Psychophysiology, University of Florida; 1988.
65. Kent JS, Michael Bailey D, Vollmer JM, et al. A magnetic resonance imaging-safe method for the study of human eyeblink conditioning. *J Neurosci Methods* 2013;216:16–21.
66. Power JD, Barnes KA, Snyder AZ, Schlaggar BL, Petersen SE. Spurious but systematic correlations in functional connectivity MRI networks arise from subject motion. *Neuroimage* 2012;59:2142–2154.
67. Diedrichsen J, Balsters JH, Flavell J, Cussans E, Ramnani N. A probabilistic MR atlas of the human cerebellum. *Neuroimage* 2009;46:39–46.
68. Diedrichsen J, Zotow E. Surface-based display of volume-averaged cerebellar imaging data. *PLoS One*. 2015;10:e0133402.
69. Tzourio-Mazoyer N, Landeau B, Papathanassiou D, et al. Automated anatomical labeling of activations in SPM using a macroscopic anatomical parcellation of the MNI MRI single-subject brain. *Neuroimage* 2002;15:273–289.
70. Maldjian JA, Laurienti PJ, Kraft RA, Burdette JH. An automated method for neuroanatomic and cytoarchitectonic atlas-based interrogation of fMRI data sets. *Neuroimage* 2003;19:1233–1239.
71. Balsters JH, Whelan CD, Robertson IH, Ramnani N. Cerebellum and cognition: evidence for the encoding of higher order rules. *Cereb Cortex* 2013;23:1433–1443.
72. Stoodley CJ, Schmahmann JD. Evidence for topographic organization in the cerebellum of motor control versus cognitive and affective processing. *Cortex* 2010;46:831–844.
73. D’Mello AM, Gabrieli JDE, Nee DE. Evidence for hierarchical cognitive control in the human cerebellum. *Curr Biol*. 2020;30:1881–1892.e3.
74. Friston K, Herreros I. Active inference and learning in the cerebellum. *Neural Comput*. 2016;28:1812–1839.
75. Moberget T, Ivry RB. Prediction, psychosis, and the cerebellum. *Biol Psychiatry Cogn Neurosci Neuroimaging* 2019;4:820–831.
76. O’Reilly JX, Mesulam MM, Nobre AC. The cerebellum predicts the timing of perceptual events. *J Neurosci*. 2008;28:2252–2260.
77. Corlett PR, Murray GK, Honey GD, et al. Disrupted prediction-error signal in psychosis: evidence for an associative account of delusions. *Brain* 2007;130:2387–2400.
78. Miller MJ, Chen NK, Li L, et al. fMRI of the conscious rabbit during unilateral classical eyeblink conditioning reveals bilateral cerebellar activation. *J Neurosci*. 2003;23:11753–11758.
79. Cheng DT, Meintjes EM, Stanton ME, et al. Functional MRI of human eyeblink classical conditioning in children with fetal alcohol spectrum disorders. *Cereb Cortex* 2017;27:3752–3767.
80. Molchan SE, Sunderland T, McIntosh AR, Herscovitch P, Schreurs BG. A functional anatomical study of associative learning in humans. *Proc Natl Acad Sci USA* 1994;91:8122–8126.
81. Parker KL, Andreasen NC, Liu D, Freeman JH, Ponto LL, O’Leary DS. Eyeblink conditioning in healthy adults: a positron emission tomography study. *Cerebellum* 2012;11:946–956.
82. Schreurs BG, McIntosh AR, Bahro M, Herscovitch P, Sunderland T, Molchan SE. Lateralization and behavioral correlation of changes in regional cerebral blood flow with classical conditioning of the human eyeblink response. *J Neurophysiol*. 1997;77:2153–2163.
83. Buckner RL, Krienen FM, Castellanos A, Diaz JC, Yeo BT. The organization of the human cerebellum estimated by intrinsic functional connectivity. *J Neurophysiol*. 2011;106:2322–2345.
84. Middleton FA, Strick PL. Cerebellar projections to the prefrontal cortex of the primate. *J Neurosci*. 2001;21:700–712.
85. Strick PL, Dum RP, Fiez JA. Cerebellum and nonmotor function. *Annu Rev Neurosci*. 2009;32:413–434.
86. King M, Hernandez-Castillo CR, Poldrack RA, Ivry RB, Diedrichsen J. Functional boundaries in the human cerebellum revealed by a multi-domain task battery. *Nat Neurosci*. 2019;22:1371–1378.